Development 128, 2031-2038 (2001)
Printed in Great Britain © The Company of Biologists Limited 2001
DEV2705

Roles of retinoic acid receptors in early embryonic morphogenesis and hindbrain patterning

Olivia Wendling, Norbert B. Ghyselinck, Pierre Chambon and Manuel Mark*

Institut de Génétique et de Biologie Moléculaire et Cellulaire (IGBMC), CNRS/INSERM/ULP/Collège de France, B.P. 163, 67404 ILLKIRCH Cedex, C.U. de STRASBOURG, France
*Author for correspondence (e-mail: marek@igbmc.u-strasbg.fr)

Accepted 13 March 2001

SUMMARY

Mutants mice carrying targeted inactivations of both retinoic acid receptor (RAR) α and RARγ (Aα/Aγ mutants) were analyzed at different embryonic stages, in order to establish the timing of appearance of defects that we previously observed during the fetal period. We show that embryonic day (E)9.5 Aα/Aγ embryos display severe malformations, similar to those already described in retinaldehyde dehydrogenase 2 null mutants. These malformations reflect early roles of retinoic acid signaling in axial rotation, segmentation and closure of the hindbrain; formation of otocysts, pharyngeal arches and forelimb buds; and in the closure of the primitive gut. The hindbrain of E8.5 Aα/Aγ embryos shows a posterior expansion of rhombomere 3 and 4 (R3 and R4) markers, but fails to express *kreisler*, a normal marker of R5 and R6. This abnormal hindbrain phenotype is strikingly different from that of embryos lacking RARα and RARβ (Aα/Aβ mutants), in which we have previously shown that the territory corresponding to R5 and R6 is markedly enlarged. Administration of a pan-RAR antagonist at E8.0 to wild-type embryos cultured in vitro results in an Aα/Aβ-like hindbrain phenotype, whereas an earlier treatment at E7.0 yields an Aα/Aγ-like phenotype. Altogether, our data suggest that RARα and/or RARγ transduce the RA signal that is required first to specify the prospective R5/R6 territory, whereas RARβ is subsequently involved in setting up the caudal boundary of this territory.

Key words: Nuclear receptors, Rhombomeres, Hox genes, *kreisler*, Embryo culture, Mouse, Vitamin A

INTRODUCTION

Retinoic acid (RA), a hormonal signal derived from vitamin A (retinol), is essential in vertebrates for controlling processes involved in embryonic patterning and organogenesis, cell proliferation, differentiation and apoptosis, and homeostasis (Sporn et al., 1994; Blomhoff, 1994; Chambon, 1996). RA levels are controlled locally, through the combined action of retinaldehyde dehydrogenases (RALDH1, RALDH2 and RALDH3) that catalyze the last step in its synthesis, and of the RA-metabolizing cytochrome P450 (CYP26) (McCaffery and Dräger, 2000; Duester, 2000; Abu-Abed et al., 2001). RA binds to nuclear receptors, the RARs (α, β and γ isotypes, that bind both all-*trans* and 9-*cis* RA) and the RXRs (α, β and γ isotypes, that bind 9-*cis* RA only), which act as transcriptional regulatory proteins mainly in the form of RAR/RXR heterodimers (Kastner et al., 1995; Chambon, 1996). The highly pleiotropic effects of RA during mammalian development have been established from the analysis of embryos and fetuses (1) obtained from females that were raised on vitamin A-deficient diets (Wilson et al., 1953; Dickman et al., 1997; White et al., 2000; Zile et al., 2000; and references therein); (2) carrying loss-of-function mutations of RARs and/or RXRs (Kastner et al., 1995; Mascrez et al., 1998; and references therein); (3) lacking the RA-generating enzyme RALDH2 (Niederreither et al., 1999); (4) lacking the RA-metabolizing enzyme CYP26 (Abu-Abed et al., 2001); (5) treated with antagonists of RARs (Wendling et al., 2000; Chazaud et al., 1999); or (6) expressing dominant-negative RARs (van der Wees et al., 1998).

An extensive functional redundancy between RARs accounts for the observation that RAR (α, β or γ)-null mutants exhibit only few developmental defects, whereas altogether the phenotypes of mutants that lack both RARα and RARβ (Aα/Aβ mutants), RARα and RARγ (Aα/Aγ mutants) and RARβ and RARγ (Aβ/Aγ mutants) recapitulate all the abnormalities characteristic of the fetal vitamin A-deficiency (VAD) syndrome (Wilson et al., 1953; Kastner et al., 1995). Of the three types of RAR double-null mutants, those that lack RARα and RARγ are overall the most severely affected. Many Aα/Aγ mutants die in utero in contrast to Aα/Aβ and Aβ/Aγ mutants, which survive until birth. Moreover, near-term (embryonic day (E)18.5) Aα/Aγ fetuses are markedly growth deficient and exhibit evident external malformations, whereas E18.5 Aα/Aβ and Aβ/Aγ fetuses are externally undistinguishable from their wild-type littermates (Lohnes et al., 1994; Mendelsohn et al., 1994; Ghyselinck et al., 1997; Luo et al., 1996).

In the first part of this work, we have established the timing of the appearance of defects previously observed in Aα/Aγ

mutants at fetal stages of development (essentially E18.5; Lohnes et al., 1994) by determining the phenotype of early embryos. Comparison of this phenotype with that of Aα/Aβ embryos (Dupé et al., 1999) has revealed major differences in the patterning of the hindbrain. In order to gain further insights into the developmental mechanisms that underlie these differences, we have studied the fate of the hindbrain when the RA-signaling pathway was blocked with a synthetic RA-antagonist, at different developmental stages.

MATERIALS AND METHODS

Mouse lines, mating and genotyping

RARα$^{+/-}$/RARγ$^{+/-}$ and RARα$^{+/-}$/RARβ$^{+/-}$/RARγ$^{+/-}$ mice were intercrossed to generate RARα$^{-/-}$/RARγ$^{-/-}$ (Aα/Aγ) and RARα$^{-/-}$/RARβ$^{+/-}$/RARγ$^{-/-}$ (Aα/Aβ$^{+/-}$/Aγ) embryos, respectively (Lufkin et al., 1993; Lohnes et al., 1993; Ghyselinck et al., 1997). Mice were mated overnight, and the next morning was considered to be 0.5 days post-coitum (E0.5). Genotyping was performed on genomic DNA from yolk sac by PCR. Primers for RARα (5′-TGTGCCCTTCCCTCCATCTTCCTTA-3′ and 5′-TCCGACTT-GCGACTCCCTCTACTCA-3′) were used to amplify a 580 bp product specific for the wild-type allele. The primer 5′-GCCTTCTATCGCCTTCTTGACGAGT-3′ was employed with the second oligo to amplify a 365 bp product specific for the disrupted allele. The PCR conditions used were 94°C for 15 seconds, 60°C for 15 seconds and 72°C for 15 seconds for 30 cycles. For RARβ genotyping, primers 5′-CCAGGCTCCTTTTTCTTCTACCATA-3′ and 5′-CTGTTTCTGTGTCATCCATTTCCAA-3′ were used to amplify a 275 bp product specific for the wild-type allele. The primer 5′-AGGCCTACCCGCTTCCATTGCTCAG-3′ was employed with the first oligo to amplify a 300 bp product specific for the disrupted allele. The PCR conditions used were 94°C for 15 seconds, 55°C for 15 seconds and 72°C for 15 seconds for 30 cycles. Primers for RARγ (5′-CAACAAGCTACAAAGAGTGGTGGTC-3′ and 5′-AAA-GCAGTTACAGGGCAGGCGAGAT-3′) were used to amplify a 1195 bp product specific for the wild-type allele. The primer 5′-GCCTTCTATCGCCTTCTTGACGAGT-3′ was employed with the second oligo to amplify a 1238 bp product specific for the mutant allele. The PCR conditions used were 94°C for 30 seconds, 57°C for 30 seconds and 72°C for 30 seconds for 30 cycles. Amplification products were resolved on 1% or 2% agarose gels and visualized by ethidium bromide staining.

Embryo culture and retinoid treatments

Embryos collected at E7.0 (primitive streak stage of gastrulation) or E8.0 (2-4 somite stages) (Kaufman, 1992; Downs and Davies, 1993), were cultured for 3 to 48 hours as described by Copp and Cockroft (1990). All-*trans*-RA (Sigma) or the pan-RAR synthetic retinoid antagonist BMS493 (Bristol-Myers-Squibb, Princeton, NJ; Wendling et al., 2000; Chazaud et al., 1999; Mollard et al., 2000), diluted in ethanol, were added to the culture medium at final concentrations of 0.1 μM for RA and 1 or 5 μM for BMS493. In control cultures, the retinoid vehicle (i.e. ethanol) was added at the same final concentration (0.1%).

External morphology, histology and in situ hybridization

Following fixation in Bouin's fluid, E9.5 embryos were rapidly rinsed in 70% ethanol, then in PBS. They were stained for 3 minutes in Acridine Orange (10 μg/ml in PBS, Sigma) (Zucker et al., 1995). Excess of stain was removed with PBS and the embryos were visualized under a fluorescence microscope (FITC filter). The embryos were postfixed in Bouin's fluid and processed for histology. Whole-mount in situ hybridization (ISH) was performed as previously described (Décimo et al., 1995) using digoxigenin-labeled riboprobes for *kreisler* (*Mafb* – Mouse Genome Informatics; Cordes and Barsh, 1994), *Krox20* (*Egr2* – Mouse Genome Informatics; Wilkinson et al., 1989), *Hoxd4* (Featherstone et al., 1988) and *EphA2* (*Epha2* – Mouse Genome Informatics; Ruiz and Robertson, 1994).

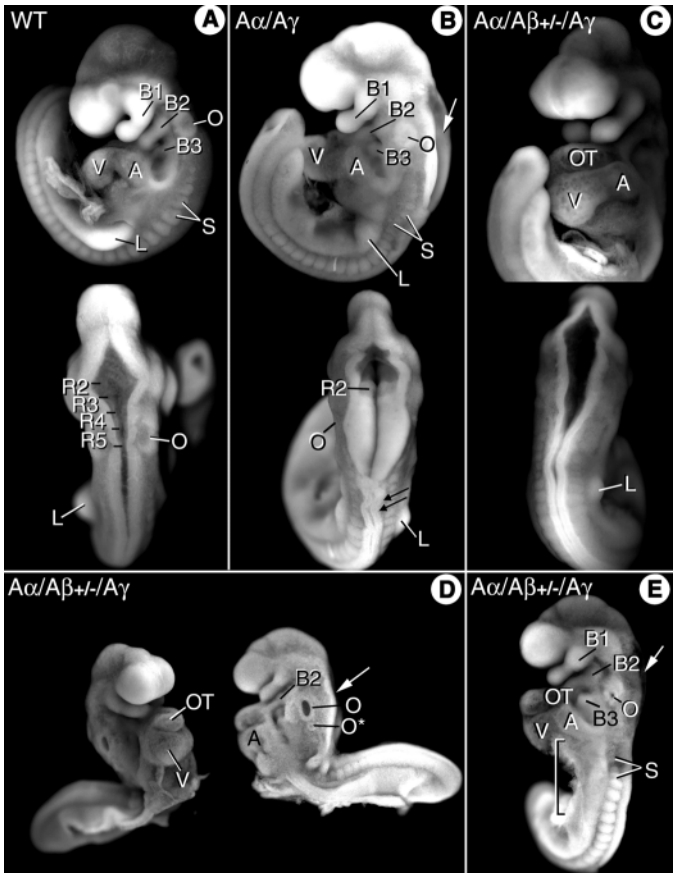

Fig. 1. Morphology of E9.5 wild type (A), Aα/Aγ (B) and Aα/Aβ$^{+/-}$/Aγ (C-E) mutants. Single arrows point to the open rhombencephalon and the double arrow to abnormal folding of the neural tube. A, heart atrium; B1-B3, pharyngeal (branchial) arches 1-3; L, limb; O and O*, orthotopic and ectopic otic vesicles; OT, heart outflow tract; R2-R5, rhombomeres 2 to 5; S, somites; V, heart ventricle. Brackets delineate the opening of the ventral body wall.

RESULTS

RARα/RARγ double-null embryos are severely malformed

At E9.5, Aα/Aγ (*n*=5) and Aα/Aβ$^{+/-}$/Aγ embryos (*n*=3) displayed a large variety of defects (compare Fig. 1A with Fig. 1B-E): axial rotation was abnormal (*n*=6/8); the anteroposterior axis was shorter (*n*=8/8); the somites were small and densely packed (*n*=8/8; compare S in Fig. 1A,B,E); the neural tube was irregularly folded at the trunk level (*n*=7/8; double arrow in Fig. 1B); the ventral body wall (*n*=8/8; brackets in Fig. 1E) and the rhombencephalic neural tube (*n*=6/8; arrow in Fig. 1B,D,E) were not closed; and the otic vesicles (*n*=6/8), forelimb buds (*n*=5/8) and second and third pharyngeal arches (*n*=2/8) were hypoplastic (compare O,L,B2, B3 in Fig. 1A,B,E). Two of the Aα/Aγ mutant hindbrains displayed two boundaries that delineated a segment located at

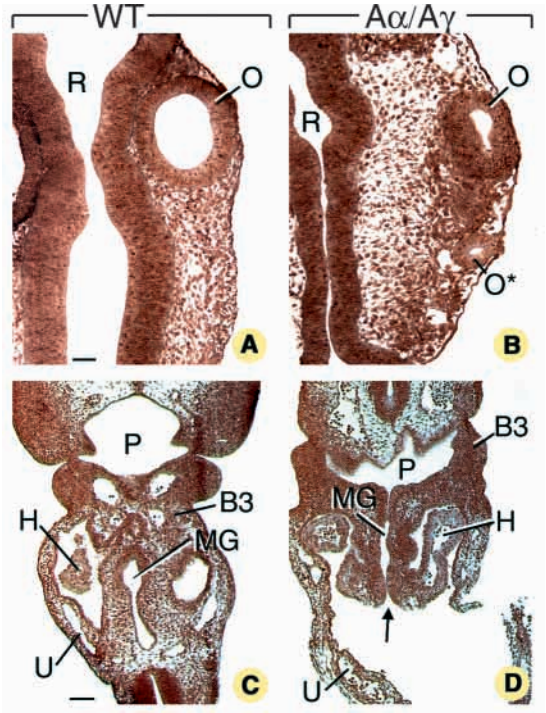

Fig. 2. Frontal histological sections at comparable levels of the hindbrain (A,B) and of the midgut (C,D) of wild type (A,C) and Aα/Aγ mutants (B,D) at E9.5. B3, branchial arch 3; H, heart; MG, midgut; O orthotopic otocyst; O*, ectopic otocyst; P, pharynx; R, rhombencephalon; U, umbilical vein. The arrow points to the persistent opening of the gut. Scale bar: 35 μm (A,B); 60 μm (C,D).

a short distance from the mesencephalic isthmus and thus identified as rhombomere 2 (R2; Fig. 1B). In all the other Aα/Aγ embryos and in the Aα/Aβ$^{+/-}$/Aγ embryos, rhombomere boundaries were completely missing (compare Fig. 1A with 1D). Except for the heart morphology (see Discussion), the external features of Aα/Aγ and Aα/Aβ$^{+/-}$/Aγ embryos are similar to those of embryos that lack retinaldehyde dehydrogenase 2 (RALDH2-null mutants) which are most probably devoid of RA (Niederreither et al., 1999). Therefore, Aα/Aγ mutants appear to reflect a state of severe functional deficiency in RA.

Histological analysis of Aα/Aγ and Aα/Aβ$^{+/-}$/Aγ embryos revealed that the deficiency in the formation of the ventral body wall affected both the ectoderm and the endoderm of the midgut (compare Fig. 2C with 2D). Four mutant embryos showed, at least on one side, and caudally to the 'main' otic vesicle (O in Figs 1A,B,D,E, 2A,B) a small cavity lined with epithelial cells (O*, Figs 1D, 2B). Similar structures previously characterized in VAD-deficient and Aα/Aβ embryos correspond to ectopic otocysts (Dupé et al., 1999; White et al., 1998).

RARα/RARγ double-null embryos lack rhombomere 5 and 6 territories

The rhombencephalic defects of Aα/Aγ mutants were further characterized at E8.5 (i.e. prior to the normal appearance of rhombomere boundaries) by in situ hybridization (ISH) analysis, using probes for three axial markers. In E8.5 wild-type embryos, *Krox20* is expressed in two well-defined stripes, the prospective R3 and R5 (pR3 and pR5; Fig. 3A; Wilkinson et al., 1989; Irving et al., 1996), which are localized at axial levels that correspond to characteristic grooves of the neural tube: the preotic and the otic sulci, respectively (PS and OS, Fig. 3A; Ruberte et al., 1997). The expression of *Hoxb1* in the rhombencephalon is restricted to pR4 (Fig. 3B; Murphy et al., 1989). Expression of *kreisler* is confined to the pR5/R6 region (Cordes and Barsh, 1994; Fig. 3C). In Aα/Aγ embryos, *Krox20* was expressed in a patchy fashion within a single broad domain that extended from the preotic sulcus to the level of the first somite (bracket in Fig. 3D). The anterior limit of *Hoxb1* expression domain was more caudal than its wild-type counterpart, relative to the preotic sulcus. Indeed this domain extended, in a patchy fashion, across the caudal hindbrain, thus largely overlapping with the abnormal *Krox20* expression domain and encompassing the region that normally corresponds to R5 and R6 ('pR4', Fig. 3E). *Hoxb1* was also ectopically expressed across the entire prospective spinal cord

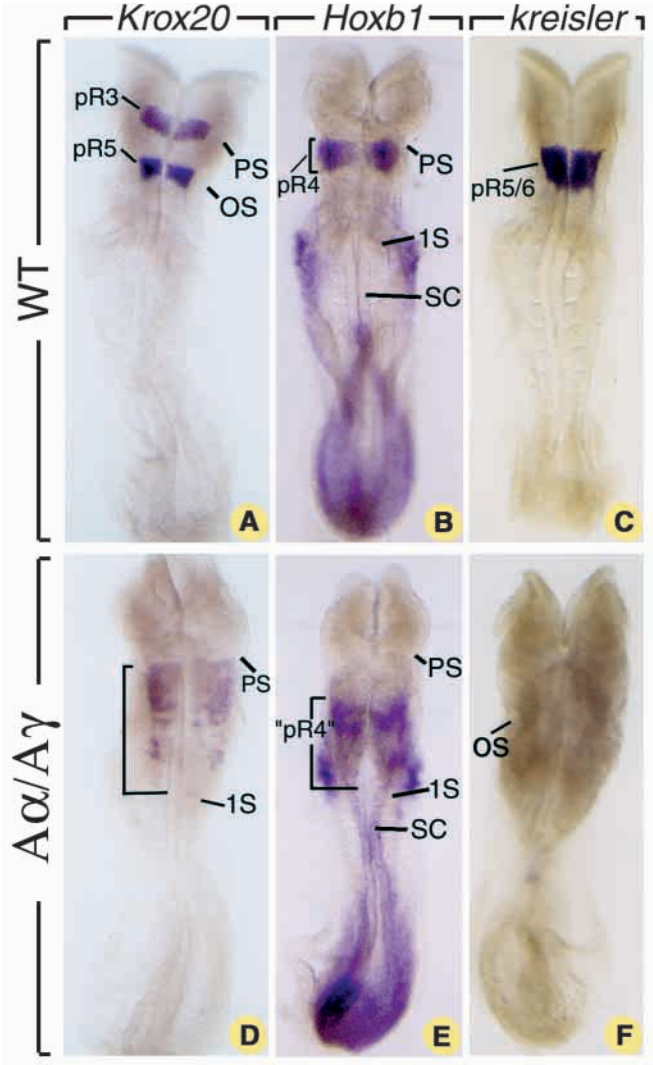

Fig. 3. Abnormal hindbrain specification in Aα/Aγ embryos. Distribution of *Krox20* (A,D); *Hoxb1* (B,E) and *kreisler* (C,F) transcripts in E8.5 wild-type (A-C) and Aα/Aγ (D-F) embryos. Dorsal views. 1S, first somite; OS, otic sulcus; pR3-pR5, pro-rhombomere 3-5; pR5/6, pro-rhombomeres 5 and 6; PS, preotic sulcus. The bracket in D encompasses the expression domain of *Krox20*.

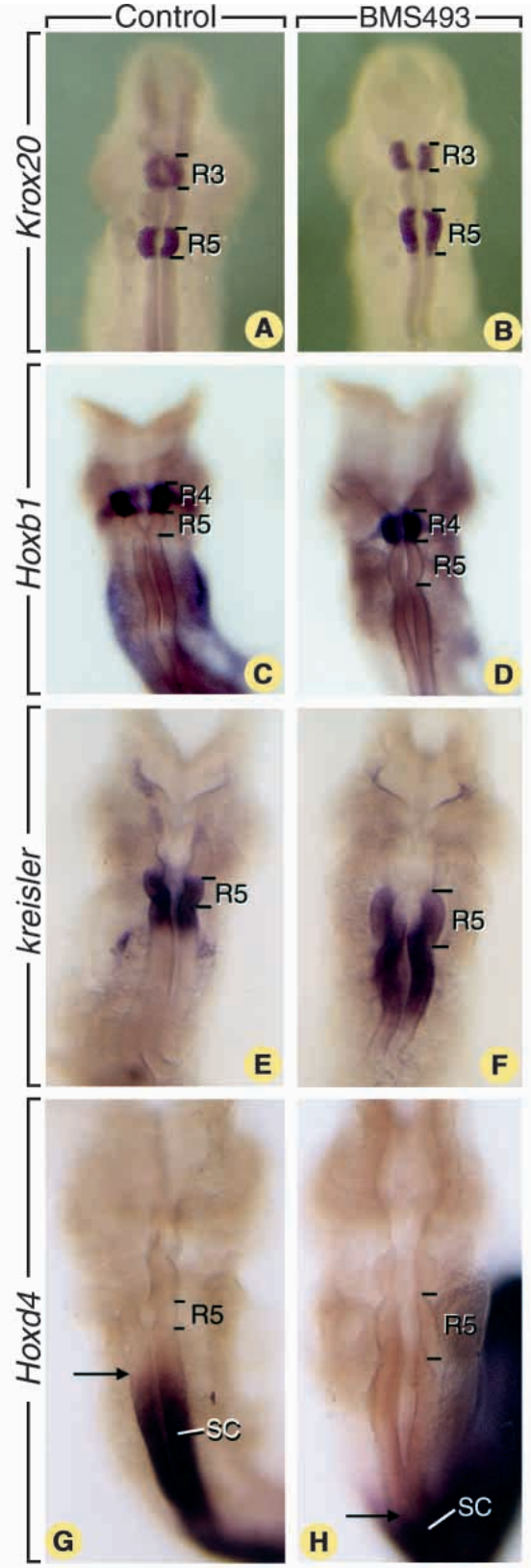

Fig. 4. Enlargement of the postotic rhombencephalon in E8+24hours BMS493-treated embryos. Distribution of *Krox20* (A,B), *Hoxb1* (C,D), *kreisler* (E,F) and *Hoxd4* (G,H) transcripts on dorsal views of cultured embryos. The arrows mark the anterior limit of *Hoxd4* transcripts in the spinal cord. R5, rhombomere 5; SC, spinal cord.

(SC, Fig. 3E). This ectopic expression resembles the normal expression of *Hoxb1* at E7.5, which extends from the prospective R3/R4 boundary up to caudal extremity of the embryo (Murphy et al., 1989). *Kreisler* transcripts were undetectable (Fig. 3F). These data indicate that the hindbrain of Aα/Aγ embryos displays a posterior expansion of R3 and R4 markers, together with loss of R5 and R6 identity.

The hindbrains of Aα/Aγ- and RALDH2-null embryos are alike, with respect to abnormalities in both morphological segmentation and expression patterns of *Krox20, Hoxb1* and *kreisler* (Niederreither et al., 1999; Niederreither et al., 2000; and see below). In contrast, these abnormalities are very different from those seen in Aα/Aβ embryos (Dupé et al., 1999; see below). This may result from differences in the timing and/or severity of the block of RA signal transduction. Alternatively or additionally, they may reflect specific functions of RARβ and RARγ in patterning distinct regions of the embryonic hindbrain. To distinguish between these possibilities, wild-type embryos collected at E8.0 (two- to four-somite stages) and E7.0 (primitive streak stage, Downs and Davies, 1993) were cultured in the presence of the pan-RAR antagonist BMS493. For convenience, the cultured embryos are referred to as E*x+y* hours BMS493-treated embryos, 'x' corresponding to the age of the embryos (in days) at the time of explantation, and 'y' to the hours spent in culture. Control embryos were exposed to the retinoid vehicle alone.

Treatment with the pan-RAR antagonist BMS493 at E8.0 generates a posterior expansion of rhombomere 5 and rhombomere 6 identities

The external morphology of the vast majority of E8.0+24 hours (*n*=70) control embryos was identical to that of E8.75 embryos in vivo (Wendling et al., 2000, and data not shown). However, in these controls, only the five rostral rhombomeres could be identified (Fig. 4A,C,E,G; data not shown). The majority of E8.0+24 hours BMS493-treated embryos (55 out of 70) showed a specific morphological enlargement of R5 (Fig. 4B,D,F,H).

The rhombomeric identities in E8.0+24 hours embryos were assessed by ISH using specific markers for R3 and R5 (*Krox20*), R4 (*Hoxb1*), R5 and R6 (*kreisler*) and R7 (*Hoxd4*). Control embryos showed reproducible patterns of transcript distribution that were identical to those seen in vivo at E8.75. *Krox20* transcripts were restricted to R3 and R5, and *Hoxb1*

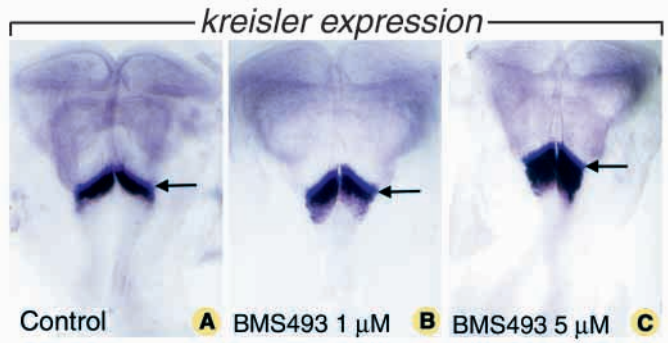

Fig. 5. RA-signaling defines the *kreisler* expression domain. E8.0 embryos cultured for 3 hours in the presence of ethanol (control, A) and BMS493 (B,C). The arrows point to the otic sulcus.

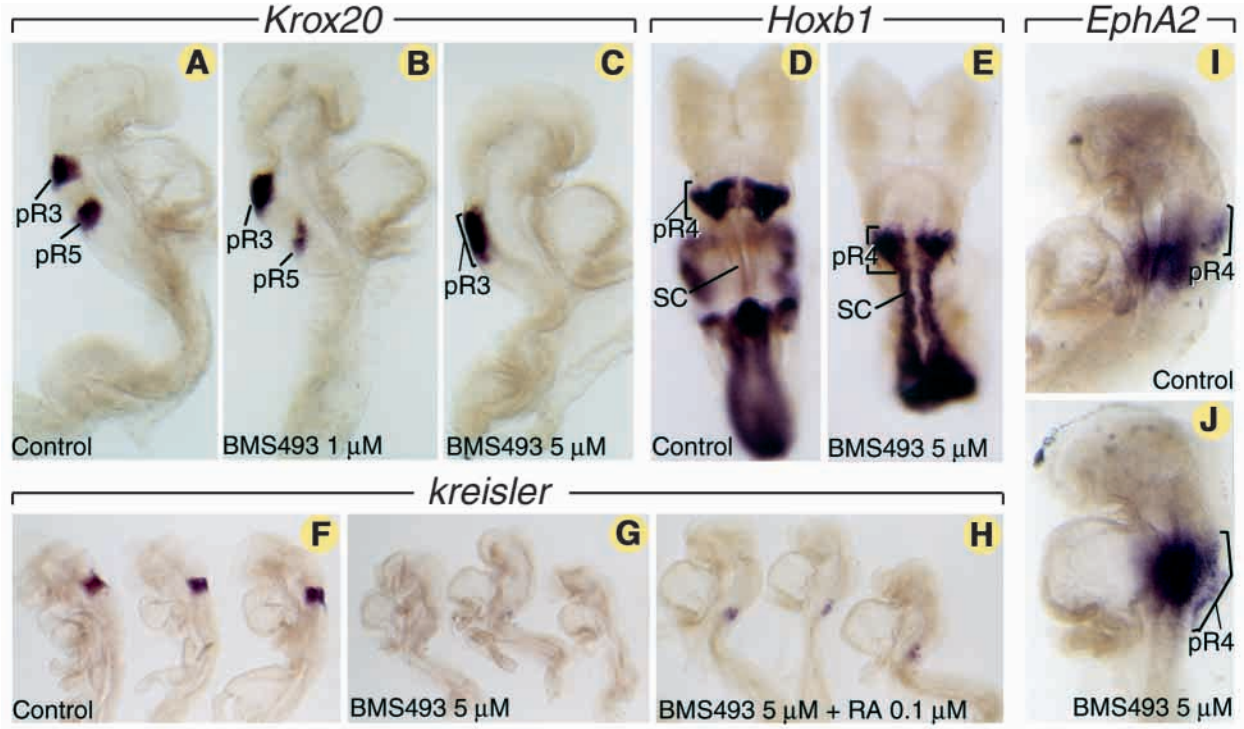

Fig. 6. Hindbrain patterning defects in E7.0 embryos cultured for 48 hours in the presence of BMS493 as indicated. Distribution of *Krox20* (A-C), *Hoxb1* (D,E), *kreisler* (F-H), *EphA2* (I,J) transcripts on lateral (A-C,F-J) and dorsal (D,E) views of cultured embryos. pR3-pR5, pro-rhombomeres 3 to 5; SC, spinal cord.

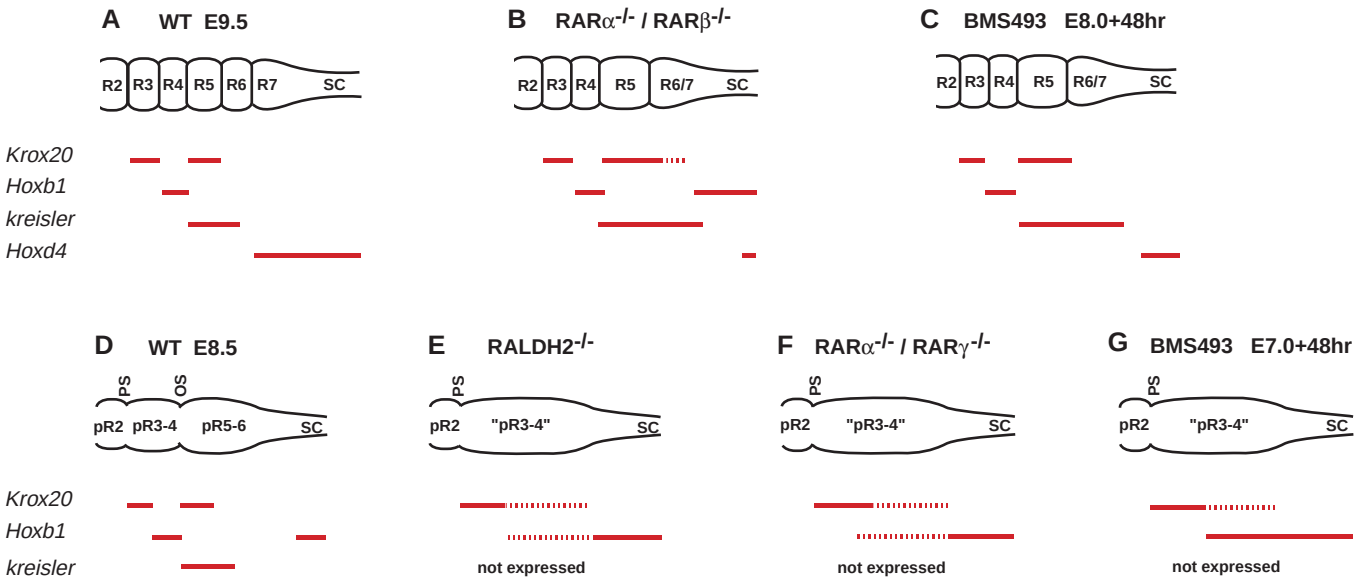

Fig. 7. Schematic representation of the morphological and molecular hindbrain patterning defects observed in various type of embryos displaying altered retinoid signalling. (A-C) Segmental expression of *Krox20*, *Hoxb1*, *kreisler* and *Hoxd4* at E9.5. (A) Wild-type embryos; (B) RARα/RARβ double-null mutant embryos (Dupé et al., 1999); (C) cultured embryos treated with the pan-RAR antagonist BMS493 at E8.0. (D-G) Segmental expression of *Krox20*, *Hoxb1* and *kreisler* at E8.5. (D) Wild-type embryos; (E) RALDH2-null mutant embryos (Niederreither et al., 2000); (F) RARα/RARγ double-null mutant embryos; (G) cultured embryos treated with BMS493 at E7.0. PS, preotic sulcus; OS, otic sulcus; R2-R7, rhombomeres 2 to 7; pR2-pR6, pro-rhombomeres 2 to 6; SC, spinal cord. The unbroken lines represent homogeneous expression of the gene, and the broken lines a patchy expression.

transcripts to R4 (Fig. 4A,C). The *kreisler* expression domain exhibited a sharp anterior limit that was coincident with the R4/R5 boundary, and a diffuse caudal limit located midway through the putative R6 (Fig. 4E; Cordes and Barsh, 1994). The anterior limit of *Hoxd4* expression was located at a distance from the R5/R6 boundary that corresponded to the length of

one rhombomere, and therefore likely matched the R6/R7 boundary (arrow in Fig. 4G; Morrison et al., 1997).

Treatments at E8.0 with 5 μM of BMS493 did not alter *Krox20* and *Hoxb1* expression in R3 and R4, respectively (Fig. 4B,D). *Krox20* and *kreisler* were expressed throughout the enlarged R5 (Fig. 4B,F), and *kreisler* expression extended more posteriorly than in controls into the R6 region (n=6/6) (compare Fig. 4E with 4F). Moreover, expression of *Hoxd4* was abolished in the hindbrain, while it remained strongly expressed in the prospective spinal cord (n=3/3; Fig. 4H). Altogether, these data indicate that a state of functional RA deficiency started at the two- to four-somite stages (i.e. about 12 hours prior to the formation of rhombomere boundaries) causes a posterior expansion of R5 and R6 characters, and the loss of an R7 character. The phenotype induced in the R3-R7 region upon treatment with BMS493 at E8.0 is clearly distinct from that of Aα/Aγ embryos, but closely related to that of Aα/Aβ embryos (Dupé et al., 1999 and see below).

To determine more precisely the time at which RA signaling is required for the determination of *kreisler* expression domain, E8.0 embryos were cultured for a short period (3 hours) in the presence of either 1 μM or 5 μM BMS493, then processed for ISH. Exposure to BMS493 resulted in a dose-dependent expansion of *kreisler* expression in the neuroectoderm caudal to the otic sulcus (arrows in Fig. 5A-C), suggesting that *kreisler* expression at E8.0 is normally repressed by RA.

Treatment with BMS493 at E7.0 induces a loss of rhombomere 5 and 6 identities

E7.0+48 hours controls (n=45) resembled E8.5 embryos developing in vivo, although they displayed abnormal folds of the spinal cord and, in 40% of the cases, severe forebrain hypoplasia. All embryos with this latter defect in control and experimental groups were discarded. E7.0+48 hours embryos treated with 5 μM BMS493 (n=37) consistently displayed a dilated heart without signs of looping or chamber formation, severe shortening of the anteroposterior axis, and small somites (compare Fig. 6A,D with 6C,E; data not shown). All these defects can be ascribed to a deficiency in RA-signaling, as a similar spectrum of defects is seen in RALDH2-null embryos (Niederreither et al., 1999; Niederreither et al., 2000; Niederreither et al., 2001).

Treatment with 5 μM BMS493, markedly enlarged the rostral stripe of *Krox20* expression caudally (compare pR3 in Fig. 6A with 6C). The *Krox20* caudal stripe (compare Fig. 6A with 6C) and the *kreisler* expression domain (Fig. 6F,G) were both absent. The pR4 was enlarged, as judged from the distribution of *EphA2* transcripts (compare pR4 in Fig. 6I with 6J; Ruiz and Robertson, 1994). The expression of *Hoxb1* was not restricted to the enlarged pR4, but instead extended throughout the spinal cord. Thus, the phenotype in the R3-R6 region induced upon treatment with BMS493 at E7.0 is very similar to that of Aα/Aγ embryos (see above).

Interestingly, in E7.0+48 hours embryos treated with a lower concentration of BMS493 (1 μM), the pR5 stripe of *Krox20* expression was reduced, whereas the pR3 stripes slightly expanded caudally (compare pR3 and pR5, Fig. 6A,B). This observation indicates that the single broad expression domain of *Krox20* observed upon treatment with 5 μM BMS493 indeed corresponds to a pR3. It also supports the view that the caudal enlargement of R3 and R4 characters in the treated embryos occurs at the expense of R5 and R6.

The loss of *kreisler* expression that occurred at E7.0 on treatment with the pan-RAR antagonist at 5 μM could be relieved upon simultaneous addition of 0.1 μM RA to the culture medium, thus demonstrating that this loss actually arose as a consequence of a block in RA signaling (Fig. 6H).

DISCUSSION

RARα and RARγ mediate early RA-dependent developmental events

The present phenotypic analysis of RARα/RARγ double-null embryos indicates that many abnormalities previously observed in E18.5 Aα/Aγ fetuses are determined prior to E9.5. This is the case for hypoplasia of forelimb skeletal elements, disruption of inner ear structures and 2nd and 3rd pharyngeal arch-derived skeletal elements, exencephaly and omphalocele (which originate from the present hypoplasia of forelimb buds, otocysts, 2nd and 3rd pharyngeal arches), and absence of closure of both the neural tube and the ventral body wall, respectively (Lohnes et al., 1994; this study).

It is noteworthy that the aforementioned defects of E18.5 Aα/Aγ mutants had not been reported in VAD animals at fetal stages of development (Wilson et al., 1953). Therefore, they might have been caused by a relief of the RA-independent transcriptional repression exerted by co-repressor-associated unliganded RAR/RXR heterodimers (reviewed in Chambon, 1996; Glass and Rosenfeld, 2000). However, the present analysis of Aα/Aγ embryos indicates that these defects actually reflect a state of RA-deficiency, as they are similar to those exhibited by RALDH2-null embryos. Indeed, RALDH2-null mutants, which lack the first RA-generating enzyme expressed during ontogenesis, are most probably devoid of RA (Niederreither et al., 1999). With one exception (see below), the spectrum of abnormalities observed in E9.5 Aα/Aγ embryos is strikingly similar to that of RALDH2-null embryos, even though some defects are either more penetrant, or more severe in these latter mutants. Indeed, axial rotation is defective in all RALDH2-null embryos, but in only a minority of Aα/Aγ embryos; the 2nd pharyngeal arch and forelimb buds are absent in RALDH2-null embryos, but severely reduced in Aα/Aγ embryos; and the entire neural tube fails to close in some RALDH2-null embryos, whereas this defect is restricted to the hindbrain in Aα/Aγ embryos.

The status of the heart represents the only notable difference between the phenotypes of Aα/Aγ and RALDH2-null mutants. In Aα/Aγ and Aα/Aβ$^{+/-}$/Aγ embryos, the heart tube shows normal (rightward) looping and displays well-defined inflow tract (including the primitive atrium; A in Fig. 1), primitive ventricle (V, Fig. 1) and outflow tract (OT, Fig. 1; O. W., N. B. G., P. C. and M. M., unpublished histological data). Likewise, Aα/Aβ embryos also display normal heart looping (Ghyselinck et al., 1997). In contrast, the heart of RALDH2-null embryos forms a medial dilated structure with poorly defined chambers, and a markedly hypoplastic inflow tract (Niederreither et al., 1999; Niederreither et al., 2001). These data suggest that the process of cardiac looping requires only low levels of signaling through RAR/RXR heterodimers, rather than a unique role of a given RAR isotype in this process. It is noteworthy that a role

of RXR homodimers in RA-mediated cardiac looping is very unlikely, as the shape of the heart is normal in mutant fetuses that lack RXR ligand-dependent transactivation functions (Mascrez et al., 1998). A block in RA-signaling transduction (BRST) generated at E7.0 through treatment with the pan-RAR antagonist, results in an absence of externally visible cardiac chambers. In contrast, the same block started at E7.5, does not alter cardiac chamber formation (Chazaud et al., 1999; Niederreither et al., 2001; Zile et al., 2000; O. W., N. B. G., P. C. and M. M., unpublished). These data suggest that, during normal embryogenesis, the cardiogenic mesoderm requires RA as early as E7.5 (i.e. prior to the appearance of the primitive medial heart tube) to form a 'loopable' primordium.

With the exception of hypoplasia of the 3rd pharyngeal arch, the defects observed in E9.5 Aα/Aγ embryos are absent in Aα/Aβ embryos. In fact, E9.5 Aα/Aβ embryos display only discrete defects, which are restricted to the caudal hindbrain (R5, R6 and R7) and pharyngeal arches 3, 4 and 6 (compare Fig. 7A with 7B; Dupé et al., 1999). Therefore, the morphogenetic effects of RA during early development (i.e. E7.5 to E9.5) are transduced by RARα and/or RARγ.

RARs are required for specification of R5 and R6 identities

Absence of rhombomere boundaries is observed upon severe RA deficiency in rats and mice (Niederreither et al., 2000; White et al., 2000), and boundaries caudal to R3 are missing in VAD quails (Gale et al., 1999). We have previously shown that the R6/R7 boundary is absent in Aα/Aβ mouse embryos (Dupé et al., 1999). Our present findings indicate that rhombomere boundaries are not formed in Aα/Aγ embryos. Altogether, these data support the view that signaling through RARs is indispensable to establish hindbrain segmentation.

The dramatic effects of RARα and γ inactivations on hindbrain segmentation can be understood in terms of mis-specification of pro-rhombomeric identities (Maden, 1999; Gavalas and Krumlauf, 2000; Barrow et al., 2000; and see below). The Aα/Aγ caudal hindbrain has apparently acquired an anterior character, as it expresses a combination of R3 and R4 molecular markers (i.e. *Krox20* and *Hoxb1*) instead of expressing *kreisler* (the earliest marker of the normal R5/R6 territory). It is noteworthy that a very similar anterior transformation of caudal hindbrain identities has been extensively documented in RALDH2-null mice (Fig. 7D-F; Niederreither et al., 1999; Niederreither et al., 2000). These observations indicate that RARα and/or RARγ mediate the RA signal required to determine the identity of R5 and R6. Interestingly, since the nucleus of the abducens nerve differentiates from the neuroectoderm of R5 and R6, the agenesis of this structure in E18.5 Aα/Aγ mutants (Lohnes et al., 1994) is likely to be a direct consequence of the absence of R5 and R6 at E8.5.

Distinct hindbrain phenotypes in RARα/RARβ and RARα/RARγ double null mutants are related to different time windows of RA action

The timecourse analysis of the alterations induced by the pan-RAR antagonist indicates that RA signaling is involved at distinct stages of the specification of the R5/R6 territory: first to permit its formation, and subsequently to define the position of its caudal boundary. A BRST generated on treatment at E7.0 yields a posterior expansion of neuroectodermal territories that carry R3 and R4 identities, and concomitant disappearance of territories that correspond to R5 and R6, leading to a phenocopy of the hindbrain patterns observed in Aα/Aγ mutants (Fig. 7D,F,G). It is noteworthy that such an early BRST is unlikely to be effective before E7.5, which corresponds to the onset of embryonic RA synthesis (Rossant et al., 1991; Ang et al., 1996; Niederreither et al., 1997). In contrast, a BRST at E8.0 does not affect the patterning of the first 4 rhombomeres, but induces a caudal expansion of territories carrying R5 and R6 identities and loss of *Hoxd4* expression in R7. Thus, a BRST at E8.0 leads to a phenocopy of hindbrain patterning defects previously described in Aα/Aβ embryos, which include apparently normal R3 and R4, an increase in the size of R5, anteriorization of R6 identity, and loss of an R7 character (i.e. *Hoxd4* expression; Dupé et al., 1999; compare Fig. 7B with 7C). RARα, RARβ and RARγ are expressed uniformly throughout the prospective hindbrain at E7.5, whereas 24 hours later, RARβ expression becomes restricted to the posterior part of this structure (Ang and Duester, 1997). Altogether these results suggest (1) that RARα and/or RARγ transduce the RA-signal that, at E7.5, is required to specify the prospective R5/R6 territory; and (2) that a caudal increase in RA-signaling at E8.0, probably mediated by RARβ, sets up the caudal boundary of this territory.

The hindbrain patterning defects observed in cultured embryos depend on the severity of the BRST. At E7.0, intermediate levels of BRST, achieved by either a low concentration of the pan-RAR antagonist or the presence of both a high concentration of this antagonist and RA, allow the formation of small domains of either *kreisler* or *Krox20* expressions. A more robust BRST abolishes the formation of these expression domains. Along the same lines, gradual enlargement of the *kreisler* expression domain parallels the level of inhibition of RA-signaling. Therefore, precise thresholds of RA signaling are apparently required to commit enough cells towards R5 and R6 fates at E7.0, and subsequently to restrict the size of the prospective R5/R6 territory at E8.0. These data suggest that the enzymatic activities, which in vivo determine RA availability (RALDHs and CYP26; Maden, 1999; Abu-Abed et al., 2001; and references therein), must be tightly controlled during the development of the embryonic hindbrain in order to generate such thresholds.

We thank Drs P. Reczek and C. Zusi for the gift of BMS493; Drs. D. Wilkinson, G. Barsh, P. Krumlauf and M. Featherstone for providing us with the cDNAs probes; and B. Féret, B. Bondeau, I. Tilly and G. Duval for technical assistance. This work was supported by funds from the Centre National de la Recherche Scientifique (CNRS), the Institut National de la Santé et de la Recherche Médicale (INSERM), the Hôpital Universitaire de Strasbourg, the Collège de France, the Institut Universitaire de France, the Association pour la Recherche sur le Cancer (ARC), the Fondation pour la Recherche Médicale (FRM), the Ligue Nationale contre le Cancer, the Human Frontier Science Program, Bristol-Myers Squibb and EEC Contract FAIR-CT97-3320. O. W. was supported by a Ligue Nationale contre le Cancer fellowship.

REFERENCES

Abu-Abed, S., Dollé, P., Metzger, D., Beckett, B., Chambon, P. and Petkovich, M. (2001). The retinoic acid-metabolizing enzyme, CYP26A1, is essential for normal hindbrain patterning, vertebral identity and development of posterior structures. *Genes Dev.* **15**, 226-240.

Ang, H. L., Deltour, L., Hayamizu, T. F., Zgombic-Knight, M. and Duester,

G. (1996). Retinoic acid synthesis in mouse embryos during gastrulation and craniofacial development linked to class IV alcohol dehydrogenase gene expression. *J. Biol. Chem.* **271**, 9526-9534.

Ang, H. L. and Duester, G. (1997). Initiation of retinoid signaling in primitive streak mouse embryos: spatiotemporal expression patterns of receptors and metabolic enzymes for ligand synthesis. *Dev. Dyn*. **208**, 536-543.

Barrow, J. R., Stadler, H. S. and Capecchi, M. R. (2000). Roles of *Hoxa1* and *Hoxa2* in patterning the early hindbrain of the mouse. *Development* **127**, 933-944.

Blomhoff, R. (ed.) (1994). *Vitamin A in Health and Disease*. New York: Marcel Dekker.

Chambon, P. (1996). A decade of molecular biology of retinoic acid receptors. *FASEB J*. **10**, 940-954.

Chazaud, C., Chambon, P. and Dollé, P. (1999). Retinoic acid is required in the mouse embryo for left-right asymmetry determination and heart morphogenesis. *Development* **126**, 2589-2596.

Copp, A. J. and Cockroft, D. L. (1990). Dissection and culture of postimplantation embryos. In *Postimplantation Mammalian Embryos: A Practical Approach*, pp. 15-40. Oxford: Oxford University Press.

Cordes, S. P. and Barsh, G. S. (1994). The mouse segmentation gene *kr* encodes a novel basic domain-leucine zipper transcription factor. *Cell* **79**, 1025-1034.

Décimo, D., Georges-Labouesse, E. and Dollé, P. (1995). *In Situ Hybridization to Cellular RNA*, pp. 183-210. New York: Oxford University Press.

Dickman, E. D., Thaller, C. and Smith, S. M. (1997). Temporally-regulated retinoic acid depletion produces specific neural crest, ocular and nervous system defects. *Development* **124**, 3111-3121.

Downs, K. M. and Davies, T. (1993). Staging of gastrulating mouse embryos by morphological landmarks in the dissecting microscope. *Development* **118**, 1255-1266.

Duester, G. (2000). Families of retinoid dehydrogenases regulating vitamin A function: production of visual pigment and retinoic acid. *Eur. J. Biochem*. **267**, 4315-4324.

Dupé, V., Ghyselinck, N. B., Wendling, O., Chambon, P. and Mark, M. (1999). Key roles of retinoic acid receptors alpha and beta in the patterning of the caudal hindbrain, pharyngeal arches and otocyst in the mouse. *Development* **126**, 5051-5059.

Featherstone, M. S., Baron, A., Gaunt, S. J., Mattei, M. G. and Duboule, D. (1988). *Hox-5.1* defines a homeobox containing gene locus on mouse chromosome 2. *Proc. Natl. Acad. Sci. USA* **85**, 4760-4764.

Gale, E., Zile, M., and Maden, M. (1999). Hindbrain respecification in the retinoid-deficient quail. *Mech. Dev.* **89**, 43-54.

Gavalas, A. and Krumlauf, R. (2000). Retinoid signalling and hindbrain patterning. *Curr. Opin. Genet. Dev*. **10**, 380-386.

Ghyselinck, N. B., Dupé, V., Dierich, A., Messaddeq, N., Garnier, J. M., Rochette-Egly, C., Chambon, P. and Mark, M. (1997). Role of the retinoic acid receptor beta (RARbeta) during mouse development. *Int. J. Dev. Biol*. **41**, 425-447.

Glass, C. K. and Rosenfeld, M. G. (2000). The coregulator exchange in transcriptional functions of nuclear receptors. *Genes Dev.* **14**, 121-141.

Irving, C., Nieto, M. A., DasGupta, R., Charnay, P. and Wilkinson, D. G. (1996). Progressive spatial restriction of *Sek-1* and *Krox-20* gene expression during hindbrain segmentation. *Dev. Biol.* **173**, 26-38.

Kastner, P., Mark, M. and Chambon, P. (1995). Nonsteroid nuclear receptors: what are genetic studies telling us about their role in real life? *Cell* **83**, 859-869.

Kaufman, M. H. (1992). *The Atlas of Mouse Development*. London: Academic Press.

Lohnes, D., Kastner, P., Dierich, A., Mark, M., LeMeur, M. and Chambon, P. (1993). Function of retinoic acid receptor gamma in the mouse. *Cell* **73**, 643-658.

Lohnes, D., Mark, M., Mendelsohn, C., Dollé, P., Dierich, A., Gorry, P., Gansmuller, A. and Chambon, P. (1994). Function of the retinoic acid receptors (RARs) during development (I). Craniofacial and skeletal abnormalities in RAR double mutants. *Development* **120**, 2723-2748.

Lufkin, T., Lohnes, D., Mark, M., Dierich, A., Gorry, P., Gaub, M. P., LeMeur, M. and Chambon, P. (1993). High postnatal lethality and testis degeneration in retinoic acid receptor alpha mutant mice. *Proc. Natl. Acad. Sci. USA* **90**, 7225-7229.

Luo, J., Pasceri, P., Conlon, R. A., Rossant, J. and Giguère, V. (1996). Compound mutants for retinoic acid receptor (RAR) beta and RAR alpha 1 reveal developmental functions for multiple RAR beta isoforms. *Mech. Dev*. **55**, 33-41.

Maden, M. (1999). Heads or tails? Retinoic acid will decide. *BioEssays* **21**, 809-812.

Mascrez, B., Mark, M., Dierich, A., Ghyselinck, N. B., Kastner, P. and Chambon, P. (1998). The RXRalpha ligand-dependent activation function 2 (AF-2) is important for mouse development. *Development* **125**, 4691-4707.

McCaffery, P. and Dräger, U. C. (2000). Regulation of retinoic acid signaling in the embryonic nervous system: a master differentiation factor. *Cytokine Growth Factor Rev*. **11**, 233-249.

Mendelsohn, C., Lohnes, D., Décimo, D., Lufkin, T., LeMeur, M., Chambon, P. and Mark, M. (1994). Function of the retinoic acid receptors (RARs) during development (II). Multiple abnormalities at various stages of organogenesis in RAR double mutants. *Development* **120**, 2749-2771.

Mollard, R., Ghyselinck, N. B., Wendling, O., Chambon, P. and Mark, M. (2000). Stage-dependent responses of the developing lung to retinoic acid signaling. *Int. J. Dev. Biol*. **44**, 457-462.

Morrison, A., Ariza-McNaughton, L., Gould, A., Featherstone, M. and Krumlauf, R. (1997). HOXD4 and regulation of the group 4 paralog genes. *Development* **124**, 3135-3146.

Murphy, P., Davidson, D. R. and Hill, R. E. (1989). Segment-specific expression of a homoeobox-containing gene in the mouse hindbrain. *Nature* **341**, 156-159.

Niederreither, K., McCaffery, P., Dräger, U. C., Chambon, P. and Dollé, P. (1997). Restricted expression and retinoic acid-induced downregulation of the retinaldehyde dehydrogenase type 2 (RALDH-2) gene during mouse development. *Mech. Dev*. **62**, 67-78.

Niederreither, K., Subbarayan, V., Dollé, P. and Chambon, P. (1999). Embryonic retinoic acid synthesis is essential for early mouse post-implantation development. *Nat. Genet.* **21**, 444-448.

Niederreither, K., Vermot, J., Schuhbaur, B., Chambon, P. and Dollé, P. (2000). Retinoic acid synthesis and hindbrain patterning in the mouse embryo. *Development* **127**, 75-85.

Niederreither, K., Vermot, J., Messaddeq, N., Schuhbaur, B., Chambon, P. and Dollé, P. (2001). Embryonic retinoic acid synthesis is essential for heart morphogenesis in the mouse. *Development* **128**, 1019-1031.

Rossant, J., Zirngibl, R., Cado, D., Shago, M. and Giguère, V. (1991). Expression of a retinoic acid response element-hsplacZ transgene defines specific domains of transcriptional activity during mouse embryogenesis. *Genes Dev.* **5**, 1333-1344.

Ruberte, E., Wood, H. B. and Morriss-Kay, G. M. (1997). Prorhombomeric subdivision of the mammalian embryonic hindbrain: is it functionally meaningful? *Int. J. Dev. Biol.* **41**, 213-222.

Ruiz, J. C. and Robertson, E. J. (1994). The expression of the receptor-protein tyrosine kinase gene, *eck*, is highly restricted during early mouse development. *Mech. Dev.* **46**, 87-100.

Sporn, M. B., Roberts, A. B. and Goodman, D. S. (eds) (1994). *The Retinoids. Biology, Chemistry and Medicine*. 2nd edn. New York: Raven Press.

van der Wees, J., Schilthuis, J. G., Koster, C. H., Diesveld-Schipper, H., Folkers, G. E., van der Saag, P. T., Dawson, M. I., Shudo, K., van der Burg, B. and Durston, A. J. (1998). Inhibition of retinoic acid receptor-mediated signalling alters positional identity in the developing hindbrain. *Development* **125**, 545-556.

Wendling, O., Dennefeld, C., Chambon, P. and Mark, M. (2000). Retinoid signaling is essential for patterning the endoderm of the third and fourth pharyngeal arches. *Development* **127**, 1553-1562.

White, J. C., Shankar, V. N., Highland, M., Epstein, M. L., DeLuca, H. F. and Clagett-Dame, M. (1998). Defects in embryonic hindbrain development and fetal resorption resulting from vitamin A deficiency in the rat are prevented by feeding pharmacological levels of all-trans-retinoic acid. *Proc. Natl. Acad. Sci. USA* **95**, 13459-13464.

White, J. C., Highland, M., Kaiser, M. and Clagett-Dame, M. (2000). Vitamin A deficiency results in the dose-dependent acquisition of anterior character and shortening of the caudal hindbrain of the rat embryo. *Dev. Biol.* **220**, 263-284.

Wilkinson, D. G., Bhatt, S., Chavrier, P., Bravo, R. and Charnay, P. (1989). Segment-specific expression of a zinc-finger gene in the developing nervous system of the mouse. *Nature* **337**, 461-464.

Wilson, J. G., Roth, C. B. and Warkany, J. (1953). An analysis of the syndrome of malformations induced by maternal vitamin A deficiency. Effects of restoration of vitamin A at various times during gestation. *Am. J. Anat.* **92**, 189-217.

Zile, M. H., Kosteskii, I., Yuan, S., Kostetskaia, E., St Amand, T. R., Chen, Y. and Jiang, W. (2000). Retinoid signaling is required to complete the vertebrate cardiac left/right asymmetry pathway. *Dev. Biol.* **223**, 323-338.

Zucker, R. M., Elstein, K. H., Shuey, D. L., Ebron-McCoy, M. and Rogers, J. M. (1995). Utility of fluorescence microscopy in embryonic/fetal topographical analysis. *Teratology* **51**, 430-434.